Genetic evidence: zebrafish *hoxba* and *hoxbb* clusters are essential for the anterior-posterior positioning of pectoral fins

Morimichi Kikuchi[a,#], Renka Fujii [a,#], Daiki Kobayashi[a,#], Yuki Kawabe[a], Haruna Kanno[a], Sohju Toyama[a], Farah Tawakkal[a], Kazuya Yamada[a], and Akinori Kawamura[a,*]

[a] Division of Life Science, Graduate School of Science and Engineering, Saitama University, Shimo-Okubo 255, Sakura-ku, Saitama 338-8570, Japan

[#]These authors equally contributed to this work.

[*]Author to whom correspondence should be addressed:
Akinori Kawamura, Ph.D.
Division of Life Science, Graduate School of Science and Engineering, Saitama University, Saitama 338-8570, Japan
Phone: +81-48-858-3808, Fax: +81-48-858-3408
E-mail: akawamur@mail.saitama-u.ac.jp

Abstract

Vertebrate paired appendages, such as the pectoral fins in fish and the forelimbs in tetrapods, emerge at specific regions along the anterior-posterior axis of the body. *Hox* genes are considered prime candidates for determining the positioning of these paired appendages during development. Despite extensive phenotypic analyses of numerous single and compound *Hox* knockout mice, no genetic studies have identified substantial defects in limb positioning, leaving questions unresolved. In a previous study, we generated seven distinct *hox* cluster-deficient mutants in zebrafish. Here, we provide genetic evidence that zebrafish *hoxba;hoxbb* cluster-deleted mutants specifically exhibit a complete absence of pectoral fins, accompanied by the absence of *tbx5a* expression in pectoral fin buds. In these mutants, *tbx5a* expression in the pectoral fin field of the lateral plate mesoderm fails to be induced at an early stage, suggesting a lack of pectoral fin precursor cells. Furthermore, the competence to respond to retinoic acid is lost in *hoxba;hoxbb* cluster mutants, indicating that *tbx5a* expression cannot be induced in the pectoral fin buds. We also identify *hoxb4a, hoxb5a, and hoxb5b* as pivotal genes underlying this process. Although the frameshift mutations in these *hox* genes do not recapitulate the absence of pectoral fins, we demonstrate that deletion mutants at these genomic loci show the absence of pectoral fins, albeit with low penetrance. Our results suggest that the positioning of zebrafish pectoral fins is cooperatively determined by *hoxb4a, hoxb5a, and hoxb5b* within *hoxba* and *hoxbb* clusters, which induce *tbx5a* expression in the restricted pectoral fin field. Our findings also provide insights into the acquisition of paired appendages in vertebrates.

Introduction

In jawed vertebrates, paired appendages—such as the pectoral and pelvic fins in fish, and their homologous forelimbs and hindlimbs in tetrapods—develop at precise locations along the anterior-posterior axis of each species. These paired appendages arise from progenitor cells located in distinct regions of the lateral plate mesoderm (Murata et al., 2010; Nishimoto and Logan, 2016; Shimada et al., 2013). The positioning of these paired appendages has long fascinated researchers, yet our understanding of the molecular mechanisms underlying this process remains limited.

In bilaterian animals, *Hox* genes—encoding evolutionarily conserved homeodomain-containing transcription factors—provide positional information and developmental timing along the anterior-posterior axis (Iimura and Pourquie, 2007; Izpisua-Belmonte and Duboule, 1992; Krumlauf, 1994). A defining feature of *Hox* genes is their structural organization into *Hox* clusters, where multiple *Hox* genes are arranged in a precise order. Additionally, *Hox* clusters exhibit a distinctive phenomenon known as *Hox* collinearity, where the genomic arrangement of *Hox* genes correlates with specific developmental regions along the body axes (Dolle et al., 1989; Duboule and Dolle, 1989; Graham et al., 1989). In vertebrates, *Hox* clusters underwent divergence due to two rounds of whole-genome duplication early in vertebrate evolution (Dehal and Boore, 2005; Ohno, 1970), leading to the establishment of four distinct *Hox* clusters (*HoxA*, *HoxB*, *HoxC*, and *HoxD*), each consisting essentially of 1-13 paralogous groups in tetrapods. In contrast, teleost fishes experienced an additional teleost-specific whole-genome duplication, followed by the loss of a *hox* cluster, resulting in seven *hox* clusters in zebrafish (Amores et al., 1998; Woltering and Durston, 2006).

Previous studies in mice and chickens suggest that the initial position of limbs is likely regulated by *Hox* genes (Tanaka, 2013; Tickle, 2015). Supporting this hypothesis, earlier research has shown that the anterior boundaries of specific *Hox* gene expression domains align with the future positions of limbs (Burke et al., 1995; Cohn et al., 1997). Moreover, experiments with avian embryos, in which several *Hox* genes were overexpressed or functionally interfered with, demonstrated altered positions of forelimb buds (Moreau et al., 2019). Additionally, it has been established that Hox proteins bind to the enhancer of *Tbx5* gene, which is crucial for the initial formation of forelimbs, thereby inducing *Tbx5* expression in the limb buds (Minguillon et al., 2012; Nishimoto et al., 2014). However, despite the generation of numerous knockout mice for single and multiple *Hox* genes, *Hoxb5* knockout mice exhibit only a rostral shift in the position of forelimb buds, with incomplete penetrance (Rancourt et al., 1995), and no significant abnormalities have been observed in the early stages of limb formation. This lack of genetic evidence for limb positioning by *Hox* genes sharply contrasts with results from genetic analyses of various knockout mice, which have shown that the paralogous 9-13 *Hox* genes in *HoxA* and *HoxD* clusters are cooperatively essential for proximal-distal patterning of limbs after limb bud formation (Boulet and Capecchi, 2004; Davis et al., 1995; Fromental-Ramain et al., 1996a; Fromental-Ramain et al., 1996b; Kmita et al., 2005). Consequently, the precise role of *Hox* genes in defining the initial position of limb formation along the anterior-posterior axis remains unclear.

Using zebrafish, which belong to the Actinopterygii class, distinct from the tetrapods of the Sarcopterygii class, we previously generated mutants lacking each of the seven zebrafish *hox* clusters using the CRISPR-Cas9 method (Yamada et al., 2021). In our recent genetic analyses of *hoxaa*, *hoxab*, and *hoxda* clusters—homologous to the

mouse *HoxA* and *HoxD* clusters—we demonstrated that, similar to mice, these zebrafish *hox* clusters cooperatively play an essential role in the formation of the pectoral fins (Ishizaka et al., 2024), which are homologous to the forelimbs. In this study, we provide the first genetic evidence, to our knowledge, that *Hox* genes specify the positions of paired appendages in the vertebrates. The double-deletion mutants of *hoxba* and *hoxbb* clusters, derived from the ancient *HoxB* cluster, exhibit a complete absence of pectoral fins due to the failure to express *tbx5a*. Despite incomplete penetrance, we propose a model in which *hoxb4a*, *hoxb5a*, and *hoxb5b* cooperatively provide positional cues along the anterior-posterior axis within the lateral plate mesoderm, thereby specifying the initial positions for fin bud formation through the induction of *tbx5a* in pectoral fin field.

Results

The absence of pectoral fins in zebrafish *hoxba;hoxbb* cluster-deleted embryos

In a previous study, we created seven individual *hox* cluster-deficient mutants in zebrafish using the CRISPR-Cas9 system (Yamada et al., 2021). Among these mutants, *hoxba* cluster-deleted embryos exhibited morphological abnormalities in their pectoral fins at 3 dpf (Figure 1A-C). To further investigate the pectoral fin phenotype in *hoxba* cluster mutants, we first analyzed the expression patterns of *tbx5a*, which plays a key role in the initial induction of pectoral fin buds in zebrafish (Ahn et al., 2002; Garrity et al., 2002; Ng et al., 2002). When comparing with *tbx5a* expression in wild-type embryos, we found that the *tbx5a* signal was reduced in the pectoral fin buds

of *hoxba* cluster mutants (Figure 1H, I). Given that *hoxba* and *hoxbb* clusters originated from the ancestral *HoxB* cluster through teleost-specific whole-genome duplication (Amores et al., 1998), there may be functional redundancy between them. Surprisingly, we discovered that the simultaneous deletion of both *hoxba* and *hoxbb* clusters resulted in the complete absence of pectoral fins (Figure 1A, G). In contrast, pectoral fins were present in *hoxba*$^{-/-}$*;hoxbb*$^{+/-}$ and *hoxba*$^{+/-}$*;hoxbb*$^{-/-}$ mutants (Figure 1E, F), indicating that an allele from either *hoxba* or *hoxbb* cluster is sufficient for the pectoral fin formation. Moreover, all embryos lacking pectoral fins were identified as *hoxba;hoxbb* double homozygous mutants, with the expected penetrance (*n*=15/252; 5.9%) being consistent with predictions based on Mendelian genetics (1/16=6.3 %). Furthermore, while *hoxba;hoxbb* cluster double homozygous mutants are embryonic lethal around 5 dpf, we could not detect any trace of pectoral fin development. Alongside this phenotype, the expression of *tbx5a* was significantly reduced to nearly undetectable levels in *hoxba;hoxbb* cluster mutants at 30 hpf (Figure 1H-M). The absence of pectoral fins in zebrafish *hoxba;hoxbb* cluster mutants sharply contrasts with the results of a previous study, which showed that mice lacking all *HoxB* genes except for *Hoxb13* of the *HoxB* cluster did not exhibit apparent abnormalities in their forelimbs (Medina-Martinez et al., 2000). Our genetic results suggest that the zebrafish *hoxba* and *hoxbb* clusters cooperatively play a crucial role in the pectoral fin formation.

Lack of pectoral fins is specific to zebrafish *hoxba;hoxbb* cluster-deleted embryos

Multiple genetic studies in mice have demonstrated the functional redundancy of *Hox* genes across the four *Hox* clusters (Horan et al., 1995; McIntyre et al., 2007; van

den Akker et al., 2001; Wellik and Capecchi, 2003; Wellik et al., 2002). To investigate whether the absence of pectoral fins is specific to *hoxba;hoxbb* cluster mutants, we created double-*hox* cluster mutants by crossing *hoxba* cluster mutants with six other *hox* cluster mutants in zebrafish. The combinatorial mutations of *hoxba* cluster with five other *hox* clusters, excluding *hoxbb* cluster, did not enhance the reduced expression of *tbx5a* (Figure 2A-H). Furthermore, we examined combined mutants of *hox* clusters, excluding *hoxba* and *hoxbb*. In *hoxca*$^{-/-}$*;hoxcb*$^{-/-}$ cluster mutants, where the functions of *HoxC* genes are completely absent, the expression patterns of *tbx5a* in fin buds were indistinguishable from those of wild-type embryos (Figure 2I). Additionally, our previous study showed that *tbx5a* expression is unaffected in *hoxaa*$^{-/-}$*;hoxab*$^{-/-}$*;hoxda*$^{-/-}$ cluster mutants (Ishizaka et al., 2024), which lack all *HoxA* and *HoxD*-related genes. The results of our deletion mutations of zebrafish *hox* clusters in various combinations emphasize that the diminished expression of *tbx5a* in the pectoral fin buds is evident only in *hoxba;hoxbb* cluster mutants. Taken together, in contrast to the functional redundancy of the four *Hox* clusters in mice, our genetic analysis indicates that the *Hox* clusters responsible for the specification of pectoral fin buds are restricted to the *HoxB*-derived *hoxba* and *hoxbb* clusters among the seven *hox* clusters in zebrafish.

Transformation of pectoral fin progenitor cells into cardiac cells in *hoxba;hoxbb* cluster-deficient embryos

To understand the absence of pectoral fin formation in *hoxba;hoxbb* cluster mutants, we examined the expression patterns of *tbx5a* during embryogenesis (Figure 3A-F). In wild-type embryos at the 10-somite stage, *tbx5a* expression appeared as bilateral symmetric stripes in the anterior lateral mesoderm, extending from the

posterior midbrain to the second somite (Figure 3A) (Ahn et al., 2002). These *tbx5a*-positive cells subsequently divided into two groups: the anteriorly migrating cells form the heart primordia, while the posteriorly migrating cells give rise to the future pectoral fin buds (Figure 3C, E). In contrast, we observed that abnormal expression patterns of *tbx5a* in the lateral mesoderm were evident at the early stages in *hoxba;hoxbb* cluster mutants. Compared to wild-type embryos, the bilateral stripes of *tbx5a* expression were shorter along the anterior-posterior axis, and the *tbx5a*-positive signal was absent from the posterior region where pectoral fin progenitor cells typically emerge (Figure 3B). Although anterior migration toward the presumptive heart occurred, posterior migration toward the fin buds was undetectable due to the lack of pectoral fin progenitor cells in *hoxba;hoxbb* cluster mutants (Figure 3D, F). These results underscore the early role of the *hoxba* and *hoxbb* clusters in providing positional information for pectoral fin buds through the induction of *tbx5a* expression. In both mice and zebrafish, there is a converse relationship between forelimb/pectoral fin and heart formation in the anterior lateral mesoderm (Keegan et al., 2005; Niederreither et al., 2001; Niederreither et al., 2002; Waxman et al., 2008). Therefore, we also analyzed cardiac development (Figure 3G-J). By examining the expression patterns of *nkx2.5*, an early cardiac progenitor marker (Chen and Fishman, 1996; Serbedzija et al., 1998), we found that the expression domain of *nkx2.5* in *hoxba;hoxbb* cluster mutants extended more posteriorly compared to wild-type embryos (Figure 3G, H). Furthermore, the region positive for the differentiated cardiac cell-specific myosin light chain (*cmlc2*) was enlarged in *hoxba;hoxbb* cluster mutants (Figure 3I, J) (Yelon et al., 1999). These results indicate that *hoxba* and *hoxbb* clusters play an essential role in the initial establishment of the pectoral fin field in zebrafish. In their absence, cells that should

form the pectoral fins instead differentiate into cardiac cells. The transformation of pectoral fin progenitor cells into cardiac cells observed in zebrafish *hoxba;hoxbb* cluster mutants is reminiscent of the anterior transformation typical of the loss-of-function phenotypes of *Hox* genes in *Drosophila* and mice (Le Mouellic et al., 1992; Lewis, 1978).

hoxba and _hoxbb_ clusters are indispensable for the retinoic acid-mediated induction of _tbx5a_ expression in the fin buds

Retinoic acid (RA) is a well-known upstream regulator of *Hox* genes in vertebrates (Boncinelli et al., 1991; Langston and Gudas, 1994; Marshall et al., 1996). Loss of function of *retinaldehyde dehydrogenase 2* (*raldh2*), an essential regulator in RA synthesis, leads to the absence of pectoral fins in zebrafish (Begemann et al., 2001; Grandel et al., 2002), a phenotype similar to that observed in *hoxba;hoxbb* cluster mutants. Previous studies have shown that exogenous RA treatments can rescue pectoral fin formation in *raldh2*$^{-/-}$ embryos (Gibert et al., 2006; Grandel et al., 2002). It has been suggested that RA directly or indirectly induces *tbx5a* expression in zebrafish fin buds (Gibert et al., 2006; Grandel and Brand, 2011; Neto et al., 2012). The phenotypic similarities between *hoxba;hoxbb* cluster mutants and *raldh2* mutants prompted us to investigate whether RA exposure could also rescue the absence of pectoral fins in *hoxba;hoxbb* cluster mutants. To explore this, we introduced a frameshift mutation in *raldh2* using CRISPR-Cas9, confirming the phenotypic recapitulation of previously described *raldh2*$^{-/-}$ mutants (figure-supplement 1). Consistent with prior results (Gibert et al., 2006; Grandel et al., 2002), RA treatment in our *raldh2* mutants rescued the expression of *tbx5a* in pectoral fins (Figure 4A-D). In contrast, RA did not induce *tbx5a*

expression in the fin buds of *hoxba;hoxbb* cluster mutants (Figure 4E-H), and no trace of pectoral fin formation was observed in the treated embryos even at 5 dpf. Furthermore, the endogenous expression patterns of *raldh2* in *hoxba;hoxbb* cluster mutants seem indistinguishable from those in wild-type embryos (Figure 4I, J), suggesting that the response to RA is absent in the fin buds of *hoxba;hoxbb* cluster mutants, while RA synthesis appears intact. Although a model proposing that RA directly induces *tbx5a* expression has been suggested (Gibert et al., 2006; Grandel and Brand, 2011; Neto et al., 2012), our results favor the model that RA-mediated induction of *tbx5a* in the fin buds occurs through *hoxba* and *hoxbb* clusters. Given that *hoxba;hoxbb* cluster mutants retain the other five intact *hox* clusters, our findings further support the notion that the *hoxba* and *hoxbb* clusters are specifically responsible for the RA-mediated specification of pectoral fins.

Expression patterns of *hoxb5a* and *hoxb5b* in pectoral fin buds are dependent on RA

The absence of pectoral fins, commonly observed in *hoxba;hoxbb* cluster mutants and *raldh2* mutants, suggests that candidate *hox* genes may be downregulated in *raldh2* mutants. To investigate this, we performed RNA-seq analysis to compare the expression profiles between sibling and *raldh2* homozygous embryos. As expected, we found that most of the 3'-located *hox* genes are downregulated in *raldh2*$^{-/-}$ embryos (Figure 5A, B, figure supplement 2). Notably, the levels of *hoxb5b* transcripts were significantly reduced, along with those of *hoxb5a* among *hoxba* genes, in *raldh2* mutants. Previous studies have shown that zebrafish *hoxb5a* and *hoxb5b* are expressed in the lateral plate mesoderm corresponding to presumptive pectoral fin buds (Waxman

et al., 2008). Additionally, knockout mice for *Hoxb5*, which is homologous to zebrafish *hoxb5a* and *hoxb5b*, only exhibit altered positioning of forelimbs (Rancourt et al., 1995), among various other *Hox* knockouts that have been generated. Therefore, we examined whether RA regulates the expression of *hoxb5a* and *hoxb5b* in fin buds. In wild-type embryos, *hoxb5a* expression was observed in the neural tube, somites, and lateral plate mesoderm (Figure 5C). However, in *raldh2* mutants, *hoxb5a* expression was significantly reduced, notably in the lateral plate mesoderm, which differentiates into the fin buds, where it was reduced to the point of being undetectable (Figure 5D). Since RA treatments in *raldh2* mutants can rescue pectoral fin development, we found that *hoxb5a* expression in *raldh2* mutants is also rescued by RA exposure (Figure 5C-E). Regarding the expression of *hoxb5b*, which diverged from the same ancestral gene as *hoxb5a*, RA-dependent expression was also confirmed, mirroring the observations made with *hoxb5a* (Figure 5F-H). These results suggest that both *hoxb5a* and *hoxb5b* are involved in the formation of the pectoral fins in zebrafish.

Genetic screening for *hox* genes responsible for the specification of pectoral fin buds in zebrafish

To understand the molecular mechanisms underlying pectoral fin specification, we aimed to identify the *hox* genes essential for pectoral fin formation through a genetic approach. By introducing frameshift mutations into the relevant *hox* genes, we anticipated that the resulting mutants would replicate the absence of pectoral fins observed in *hoxba;hoxbb* mutants. Since *hoxbb* cluster contains fewer *hox* genes than *hoxba* cluster (Figure 5A), we focused our investigation on *hoxbb* cluster. Although *hoxb5b* is expressed in the presumptive fin buds (Figure 5F), other *hoxbb* genes may

also be involved. Therefore, we simultaneously injected three gRNAs targeting *hoxb5b*, *hoxb6b*, and *hoxb8b* into *hoxba* hemizygous mutants, expecting various germline mutations in these *hoxbb* genes in the injected fish (Figure 6A). Subsequently, F1 fish with a hemizygous deletion of *hoxba* cluster and mosaic mutations were crossed with *hoxba;hoxbb* hemizygous mutants. Among the progeny, several embryos lacking pectoral fins were identified. Following genotyping and DNA sequencing of the target *hoxbb* genes, we found that all embryos without pectoral fins possessed frameshift mutations in *hoxb5b*, with *hoxba*$^{-/-}$*;hoxbb*$^{+/-}$ being common among them (Figure 6B-E, table-supplement 1, figure-supplement 3). Similarly, we injected each crRNA for *hoxb6b* and *hoxb8b* into *hoxba*$^{+/-}$ mutants and confirmed that neither frameshift mutation in *hoxb6b* nor *hoxb8b* in *hoxba*$^{-/-}$*;hoxbb*$^{+/-}$ led to the loss of pectoral fins (Figure 6F, G, figure-supplement 3). These results suggest that the frameshift mutation of *hoxb5b* alone can compensate for the deletion of *hoxbb* cluster, recapitulating the absence of pectoral fins in *hoxba;hoxbb* cluster mutants.

However, we encountered a problem: *hoxba*$^{-/-}$*;hoxb5b*$^{-/-}$ embryos, which have a homozygous frameshift mutation in *hoxb5b* and a homozygous deletion of *hoxba* cluster, exhibited severely truncated but visibly present pectoral fins (Figure 6H, I). After analyzing hundreds of embryos from several crossings, we did not find any *hoxba*$^{-/-}$*;hoxb5b*$^{-/-}$ embryos without pectoral fins. We also confirmed that the expression of *tbx5a* was detectable in the fin buds of *hoxba*$^{-/-}$*;hoxb5b*$^{-/-}$ embryos (Figure 6K, L), in contrast to its absence in *hoxba;hoxbb* cluster mutants (Figure 1M). To examine the potential contributions of other *hoxbb* genes, we observed the phenotypes of *hoxba*$^{-/-}$*;hoxb5b*$^{-/-}$*; hoxb6b*$^{-/-}$ embryos; however, these mutants did not exacerbate the abnormalities and did not also exhibit the absence of pectoral fins (Figure 6J, M).

The phenotype of *hoxba*$^{-/-}$*;hoxb5b*$^{-/-}$ embryos indicates that the frameshift mutation in *hoxb5b* cannot fully compensate for the complete deletion of *hoxbb* cluster, suggesting that other mechanisms may be involved. A novel genetic compensation mechanism known as transcriptional adaptation has been identified: mRNA containing a premature termination codon (PTC) can induce increased expression of structurally related genes, thereby compensating for the function of mutated genes (El-Brolosy et al., 2019; Rossi et al., 2015). To avoid producing transcripts with PTC (Sztal and Stainier, 2020), we generated a full locus-deleted allele of *hoxb5b* using CRISPR-Cas9 with two crRNAs targeting both ends of the target locus (figure-supplement 4). In contrast to the phenotype of *hoxba*$^{-/-}$*;hoxb5b*$^{-/-}$, we found that *hoxba*$^{-/-}$*;hoxb5b* $^{de/dell}$ mutants lack pectoral fins and exhibit a significant reduction in *tbx5a* expression when intercrossing *hoxba*$^{+/-}$*;hoxb5b*$^{+/del}$ fish (Figure 7A, B, D, E). However, the occurrence rate of embryos lacking pectoral fins (*n*=3/120; 2.5 %) was lower than predicted based on Mendelian genetics (1/16; 6.3 %). Other *hoxba*$^{-/-}$*;hoxb5b*$^{del/del}$ embryos did exhibit shortened pectoral fins (Figure 7C). Additionally, concerning *hoxba* cluster, we also generated frameshift-induced *hoxb5a*$^{-/-}$*;hoxb5b*$^{-/-}$ and a full locus-deleted *hoxb5a*$^{del/del}$*;hoxb5b*$^{del/del}$ embryos (figure-supplement 4). *hoxb5a*$^{-/-}$*;hoxb5b*$^{-/-}$ larvae consistently displayed normal pectoral fins (Figure 7F). In contrast, *hoxb5a*$^{del/del}$*;hoxb5b*$^{del/del}$ mutants exhibited a slightly more pronounced phenotype of shortened pectoral fins, but no instances of missing pectoral fins were identified (Figure 7G). Furthermore, due to the functional redundancy observed between *hoxb4a* and *hoxb5a* observed in zebrafish vertebral patterning and the RA-dependent expression of *hoxb4a* (Grandel et al., 2002; Maeno et al., 2024), as well as its expression in fin buds (Figure 7H), we generated frameshift-induced *hoxb4a*$^{-/-}$*;hoxb5a*$^{-/-}$*;hoxb5b*$^{-/-}$ embryos and an allele lacking the entire

genomic region encompassing *hoxb4a* and *hoxb5a* (figure-supplement 4). Although *hoxb4a*$^{-/-}$;*hoxb5a*$^{-/-}$;*hoxb5b*$^{-/-}$ embryos did not lack pectoral fins (Figure 7I), some *hoxb4a-b5a*$^{del/del}$;*hoxb5b*$^{del/del}$ embryos did lack pectoral fins, although at low penetrance (Figure 7J, *n*=3/397; 0.7%). The majority of *hoxb4a-b5a*$^{del/del}$;*hoxb5b*$^{del/del}$ embryos displayed truncated pectoral fins (Figure 7K). The lack of pectoral fins was not detected in *hoxb4a-b5a*$^{del/del}$ and *hoxb4a*$^{del/del}$;*hoxb5b*$^{del/del}$ mutants (Figure 7L, M, (figure-supplement 4). These results suggest that *hoxb4a*, *hoxb5a*, and *hoxb5b* may cooperatively contribute to anterior-posterior positioning of pectoral fin buds in zebrafish. Furthermore, our findings reveal that transcriptional adaptation may partially play a role in genetic compensation for frameshift-induced *hox* mutations during pectoral fin formation, while also suggesting the potential involvement of other unknown mechanisms or additional genomic regions in the initial induction of zebrafish pectoral fin buds.

Discussion

Since the establishment of gene targeting (Mansour et al., 1988), numerous *Hox* knockout mice have been generated. However, neither single nor compound *Hox* mutants, nor *Hox* overexpression approaches, have been reported to cause significant defects in limb positioning (Jurberg et al., 2013; Moreau et al., 2019). Consequently, the role of *Hox* genes in the positioning of vertebrate paired appendages remains unclear due to a lack of genetic evidence. In this study, we provide genetic evidence using zebrafish, demonstrating that specific combinatorial deletions of *hoxba* and *hoxbb* clusters result in the absence of pectoral fins and a lack of induction of *tbx5a* expression

in the pectoral fin field. Based on our results, we propose a model in which *Hox* expressions in the lateral plate mesoderm, regulated by RA synthesized in the paraxial mesoderm, provide positional information and induce *tbx5a* expression in the presumptive fin buds. Our genetic results shed light on longstanding fundamental questions regarding the molecular mechanisms by which the positioning of paired appendages is established in vertebrates.

Zebrafish *hoxba* and *hoxbb* clusters, possibly *hoxb4a*, *hoxb5a*, and *hoxb5b*, cooperatively define the pectoral fin field in the lateral plate mesoderm.

We showed that *hoxba;hoxba* mutants exhibit a lack of pectoral fins. The abnormal expression of *tbx5a* in the lateral plate mesoderm, where pectoral fin precursor cells arise, was evident from its initial expression in the mutants. We presume that *hox* genes in *hoxba* and *hoxbb* clusters, induced by RA, define the region along the anterior-posterior axis where pectoral fin formation can occur and promote the expression of *tbx5a* in the lateral plate mesoderm. Importantly, *tbx5a* expression in the fin bud was not induced even by RA exposure in *hoxba;hoxbb* mutants (Figure 4E-H). In zebrafish, it has been suggested that RA synthesized in the paraxial mesoderm acts directly on the lateral plate mesoderm, or that RA induces *tbx5a* expression via *wnt2b* in the intermediate mesoderm (Gibert et al., 2006; Grandel and Brand, 2011; Neto et al., 2012). However, our results suggest that the main pathway integrates these signaling cascades through *hoxba* and *hoxbb* clusters to induce *tbx5a* expression. Through genetic studies, despite low penetrance, we showed that *hoxb4a*, *hoxb5a*, and *hoxb5b* play a significant role in the induction of pectoral fin buds. The homologous Hoxb4 and

Hoxb5 proteins in mice have been shown to bind directly to the enhancer of *Tbx5* (Minguillon et al., 2012). Furthermore, it has been demonstrated that the *Tbx5* expression in the forelimb field is restricted by the posterior *Hox* genes, preventing posterior expansion in mice and chickens (Moreau et al., 2019; Nishimoto et al., 2014). However, our several combinatorial deletions of zebrafish *hox* clusters did not exhibit any abnormalities in which the expression of *tbx5a* expanded to the posterior. Therefore, in zebrafish, we propose that *hoxb4a*, *hoxb5a*, and *hoxb5b*, which are induced by RA in the lateral plate mesoderm, simply upregulate the expression of *tbx5a*.

Partial recapitulation of genomic locus-deleted *hox* mutants suggests the other unidentified mechanisms.

In this study, we observed that *hox* mutants with deletions of genomic loci exhibited more pronounced pectoral fin phenotypes than frameshift-induced *hox* mutants. The frameshift mutants used in this study are likely to be loss-of-function alleles, as we demonstrated several defects in vertebral patterning in these mutants (Maeno et al., 2024). These results suggest that transcriptional adaptation may occur during the formation of pectoral fins in frameshift-induced *hox* mutants, potentially compensating for the loss of function. In our previous studies, which focused on dorsal and anal fin patterning, vertebral patterning, and swim bladder formation, we demonstrated that the phenotypes observed in zebrafish *hox* cluster-deleted mutants could essentially be replicated by introducing frameshift mutations into *hox* genes within the cluster (Adachi et al., 2024; Maeno et al., 2024; Satoh et al., 2024; Yamada et al., 2021). Therefore, creating a mutant with a deleted locus that does not induce

transcriptional adaptation was unnecessary. One factor that may explain the differences in results between this study and our prior findings is that even a small amount of *hox* gene products essential for pectoral fin positioning may be sufficient to induce fin buds, as shown in Figure 1, potentially leading to the manifestation of gene compensation through transcriptional adaptation in frameshift-induced mutants. Alternatively, transcriptional adaptation may function differently depending on various developmental processes or stages. Interestingly, all the aforementioned phenotypes reproducible by frameshift mutations were observed at later developmental stages than pectoral fin formation. Additionally, in *hox* locus-deleted mutants, only some *hoxba*$^{-/-}$;*hoxb5b*$^{de/dell}$ or *hoxb4a-b5a*$^{del/del}$;*hoxb5b*$^{del/del}$ embryos were able to reproduce the loss of the pectoral fin, suggesting the presence of other compensatory mechanisms. The organized expression patterns of *Hox* genes are thought to be regulated by complex regulatory controls, with their expression regulated according to the genomic order within the cluster. In the absence of *Hox* function, neighboring intact *Hox* genes could compensate for the loss of function. It is also possible that unidentified non-coding regions in *hoxba* and *hoxbb* clusters are involved in pectoral fin positioning. These issues should be clarified in future studies.

Hox genes may have contributed to the acquisition of pectoral fins during vertebrate evolution.

According to fossil records from the Cambrian period, the most primitive vertebrates did not possess paired fins (Janvier, 1996; Shubin et al., 1997). It is believed that, during subsequent evolution, vertebrates acquired primitive pectoral and pelvic

fins, which served as evolutionary precursors to tetrapod limbs, before diverging into ray-finned and lobe-finned fishes. Our results align well with this evolutionary scenario. *Hox* genes, which are conserved in bilaterian animals, are thought to have been present in primitive vertebrates without paired fins. The early fossils of vertebrates with pectoral fins were discovered in Ordovician and Silurian jawless fish (Janvier, 1996; Shubin et al., 1997). Since it is estimated that two rounds of whole-genome duplications occurred early in the Cambrian period (Dehal and Boore, 2005), the first vertebrate with pectoral fins likely possessed four sets of *Hox* clusters, similar to those found in modern tetrapods. *Hox* genes have long been fundamental tools for animal development, even before vertebrates acquired paired fins. The acquisition of new functions in specific *Hox* genes may have contributed to the innovation of novel morphological features. Our findings that *hoxba;hoxbb* mutants completely lack pectoral fins suggest that molecular evolution within the ancestral *HoxB* cluster may have contributed to the development of pectoral fins in vertebrates. Although the specific molecular modifications remain unclear, one possible model suggests that *HoxB* gene(s) acquired a new capacity to induce the expression of *Tbx5* in the lateral plate mesoderm. This may have played a role in establishing the RA-*HoxB*-*Tbx5* gene cascade, which is essential for pectoral fin formation. Notably, the ancestral *Tbx4/5* in ascidians, which do not have paired fins, already possesses the ability to rescue the loss of forelimbs in mice (Minguillon et al., 2009). Consistent with our idea, a model has been proposed in which the induction of *Tbx5* in the lateral plate mesoderm may have contributed to the acquisition of pectoral fins.

Since *hoxba;hoxbb* mutants are embryonic lethal around 5 dpf, we cannot observe the effects of these clusters on the pelvic fins, which develop around one month

after fertilization in zebrafish (Parichy et al., 2009). However, based on the composition of zebrafish *hox* genes and their expression patterns in *hoxba* and *hoxbb* clusters, we presume that these clusters have functions specific to the positioning of pectoral fins. The presence of *hox* genes responsible for the position of pectoral fins implies that there may be other *hox* genes that determine the position of pelvic fins and possibly contribute to their acquisition. This remains a critical area for future research.

The positioning of pectoral fins is restricted to specific *hox* clusters in zebrafish, in contrast to the functional overlap seen in mice.

Taking advantage of our availability of seven individual *hox* cluster mutants in zebrafish, we created mutants with multiple cluster deletions. Through genetic analysis, we demonstrated that *hox* genes responsible for positioning pectoral fin buds are restricted to *hoxba* and *hoxbb* clusters. In contrast, analyses of knockout mice reveal significant functional overlap among the four *Hox* clusters. Mice lacking all *HoxB* genes except for *Hoxb13* have been generated, yet there are no reports of a phenotype characterized by absent forelimbs (Medina-Martinez et al., 2000). In *Hoxb5* knockout mice, the position of the forelimbs shifts rostrally by one vertebra, and forelimbs are not absent in *Hoxa5;Hoxb5;Hoxc5* triple knockout mice, which lack all *Hox* genes of the paralog 5 group (Xu et al., 2013). In comparison, zebrafish *hoxba;hoxbb* mutants exhibit a striking phenotype of absent pectoral fins. This phenomenon, where function is confined to specific *hox* clusters, has also been observed in other developmental systems of teleosts. In both zebrafish and medaka, multiple *hox* genes responsible for positioning dorsal and anal fins are primarily located in *HoxC*-related clusters (Adachi

et al., 2024). As mentioned earlier, it is believed that paired fins in vertebrates emerged after the quadruplication of the primitive *Hox* clusters. Therefore, *Hox* genes that acquired new functions related to pectoral fin formation likely originated from specific *Hox* clusters among the four, maintaining restricted functions that diverged after the teleost-specific whole-genome duplication. The validity of this assumption requires further verification through a clearer understanding of the overall functions of the 49 *hox* genes in zebrafish. However, the genetic results thus far suggest that, unlike in mice, the functions of *hox* genes—especially those related to development uniquely acquired in vertebrates—may be confined to specific *hox* clusters in zebrafish. While teleosts have gained functional redundancy through subsequent teleost-specific whole-genome duplication, it is postulated that, in mice, which have maintained four *Hox* clusters for over half a billion years, functional overlap among *Hox* genes may ensure the robustness of the developmental system.

Materials and methods

Zebrafish

Riken Wild-type (RW) zebrafish, obtained from the National BioResource Project in Japan, were maintained at 27°C with a 14-hour light/10-hour dark cycle. Embryos were collected from natural spawning, and the larvae were raised at 28.5°C. Developmental stages of the embryos and larvae were determined based on hours post-fertilization (hpf), days post-fertilization (dpf), and developmental stage-specific features (Kimmel et al., 1995; Parichy et al., 2009). The alleles of *hox* cluster-deleted mutants used in this study were previously generated using CRISPR-Cas9 (Yamada et al., 2021). The following frameshift-induced *hox* mutants were created using CRISPR-Cas9: *hoxb5a*^{sud125}, *hoxb5b*^{sud136}, *hoxb6b*^{sud137}, and *hoxb4a;hoxb5a*^{sud144} (Maeno et al., 2024). All experiments involving live zebrafish were approved by the Committee for Animal Care and Use of Saitama University.

Generation of mutants by the CRISPR-Cas9 system

All the mutants used in this study were generated using the Alt-R CRISPR-Cas9 system (Integrated DNA Technologies). To create frameshift-induced mutants, gene-specific crRNAs were incubated with common tracrRNA, followed by Cas9 nuclease. For the generation of mutants that delete large genomic regions, two crRNAs targeting both ends of the regions were incubated with common tracrRNA and Cas9 nuclease. Approximately one nanoliter of the crRNA:tracrRNA-Cas9 RNA-protein complex was injected into fertilized embryos, which were subsequently raised to juvenile fish. Candidate founder fish were selected using a heteroduplex

mobility shift assay for frameshift mutants (Ota et al., 2013) and by amplifying genomic deletions with specific primers. After sexual maturation, candidate founder fish were mated with wild-type fish to produce heterozygous F1 offspring. Among the F1 offspring, mutant fish carrying the same mutation were identified through PCR-based genotyping followed by DNA sequencing. The target-specific sequences of the crRNAs used in this study are listed (table-supplement 2). The frozen sperms from the mutants used in this study have been deposited in the National BioResource Project Zebrafish in Japan (https://shigen.nig.ac.jp/zebra/) and are available upon request.

Genotyping of mutants

For the phenotypic analysis of embryos and the maintenance of mutant fish lines, PCR-based genotyping was performed. Briefly, genomic DNA was extracted from the analyzed embryos or the partially dissected caudal fins of anesthetized larvae or fish using the NaOH method (Meeker et al., 2007), which served as the template for PCR. The sequences of the primers used for genotyping frameshift-induced mutants are listed in the supplementary Table 3. For genotyping deletion mutants of *hox* genes, PCR was conducted using a combination of three primers, with their sequences also provided (table-supplement 3). Genotyping of *hox* cluster-deleted mutants was performed using PCR as previously described (Yamada et al., 2021). After the reactions, the PCR products were separated by electrophoresis. Based on differences in the lengths of PCR products derived from wild-type and mutated alleles, either a 2 % agarose gel in 0.5x TBE buffer, a 15 % polyacrylamide gel in 0.5x TBE buffer, or direct DNA sequencing was utilized to determine the genotype.

Whole-mount *in situ* hybridization

Whole-mount *in situ* hybridization was carried out as described (Thisse and Thisse, 2014). After the staining, the embryos mounted in 70-80 % glycerol were captured under the stereomicroscope (Leica M205 FA) with a digital camera (Leica DFC350F). After taking images, PCR-based genotyping was carried out as described above.

RNA-seq analysis

For RNA-seq analysis, embryos were obtained by the intercrosses between *raldh2* heterozygous fish. At the 18-20-somite stages, sibling and homozygous embryos were separated based on the phenotype, and 20 embryos per tube were collected. Then, total RNA was extracted by ISOGENE (Nippon Gene) and followed by DNase I treatment (Takara). After the quality check of the isolated RNA, RNA-seq analyses (n=2 for each) were carried out by Genewiz, Azenta Life Science.

Treatment of retinoic acid in the embryos

Treatment of retinoic acid on the embryos was performed as previously described, with minor modifications (Gibert et al., 2006; Grandel et al., 2002). Briefly, embryos were obtained from intercrosses between *raldh2* heterozygous mutants. At the 70 % epiboly stage, the embryos were soaked in a solution containing DMSO or 10^{-8}M RA and incubated at 28.5°C. Embryos were fixed at 30 hpf for analysis of *tbx5a* expression and at the 10-somite stage for examination of *hox* gene expression.

Acknowledgments

We thank the NBRP zebrafish for providing fish and preserving the mutant lines generated in this study. We also appreciate Drs. Koji Tamura and Gembu Abe for providing the zebrafish *tbx5a* plasmid. This work was supported by KAKENHI Grants-in-Aid for Scientific Research 18K06177, 23K05790 to AK.

References

Adachi, U., Koita, R., Seto, A., Maeno, A., Ishizu, A., Oikawa, S., Tani, T., Ishizaka, M., Yamada, K., Satoh, K., et al. (2024). Teleost Hox code defines regional identities competent for the formation of dorsal and anal fins. *Proc Natl Acad Sci U S A* **121**, e2403809121.

Ahn, D. G., Kourakis, M. J., Rohde, L. A., Silver, L. M. and Ho, R. K. (2002). T-box gene tbx5 is essential for formation of the pectoral limb bud. *Nature* **417**, 754-758.

Amores, A., Force, A., Yan, Y. L., Joly, L., Amemiya, C., Fritz, A., Ho, R. K., Langeland, J., Prince, V., Wang, Y. L., et al. (1998). Zebrafish hox clusters and vertebrate genome evolution. *Science* **282**, 1711-1714.

Begemann, G., Schilling, T. F., Rauch, G. J., Geisler, R. and Ingham, P. W. (2001). The zebrafish neckless mutation reveals a requirement for raldh2 in mesodermal signals that pattern the hindbrain. *Development* **128**, 3081-3094.

Boncinelli, E., Simeone, A., Acampora, D. and Mavilio, F. (1991). HOX gene activation by retinoic acid. *Trends Genet* **7**, 329-334.

Boulet, A. M. and Capecchi, M. R. (2004). Multiple roles of Hoxa11 and Hoxd11 in the formation of the mammalian forelimb zeugopod. *Development* **131**, 299-309.

Burke, A. C., Nelson, C. E., Morgan, B. A. and Tabin, C. (1995). Hox genes and the evolution of vertebrate axial morphology. *Development* **121**, 333-346.

Chen, J. N. and Fishman, M. C. (1996). Zebrafish tinman homolog demarcates the heart field and initiates myocardial differentiation. *Development* **122**, 3809-3816.

Cohn, M. J., Patel, K., Krumlauf, R., Wilkinson, D. G., Clarke, J. D. and Tickle, C. (1997). Hox9 genes and vertebrate limb specification. *Nature* **387**, 97-101.

Davis, A. P., Witte, D. P., Hsieh-Li, H. M., Potter, S. S. and Capecchi, M. R. (1995). Absence of radius and ulna in mice lacking hoxa-11 and hoxd-11. *Nature* **375**, 791-795.

Dehal, P. and Boore, J. L. (2005). Two rounds of whole genome duplication in the ancestral vertebrate. *PLoS Biol* **3**, e314.

Dolle, P., Izpisua-Belmonte, J. C., Falkenstein, H., Renucci, A. and Duboule, D. (1989). Coordinate expression of the murine Hox-5 complex homoeobox-containing genes during limb pattern formation. *Nature* **342**, 767-772.

Duboule, D. and Dolle, P. (1989). The structural and functional organization of the murine HOX gene family resembles that of Drosophila homeotic genes. *EMBO J* **8**, 1497-1505.

El-Brolosy, M. A., Kontarakis, Z., Rossi, A., Kuenne, C., Gunther, S., Fukuda, N., Kikhi, K., Boezio, G. L. M., Takacs, C. M., Lai, S. L., et al. (2019). Genetic compensation triggered by mutant mRNA degradation. *Nature* **568**, 193-197.

Fromental-Ramain, C., Warot, X., Lakkaraju, S., Favier, B., Haack, H., Birling, C., Dierich, A., Doll e, P. and Chambon, P. (1996a). Specific and redundant functions of the paralogous Hoxa-9 and Hoxd-9 genes in forelimb and axial skeleton patterning. *Development* **122**, 461-472.

Fromental-Ramain, C., Warot, X., Messadecq, N., LeMeur, M., Dolle, P. and Chambon, P. (1996b). Hoxa-13 and Hoxd-13 play a crucial role in the patterning of the limb autopod. *Development* **122**, 2997-3011.

Garrity, D. M., Childs, S. and Fishman, M. C. (2002). The heartstrings mutation in zebrafish causes heart/fin Tbx5 deficiency syndrome. *Development* **129**, 4635-4645.

Gibert, Y., Gajewski, A., Meyer, A. and Begemann, G. (2006). Induction and prepatterning of the zebrafish pectoral fin bud requires axial retinoic acid signaling. *Development* **133**, 2649-2659.

Graham, A., Papalopulu, N. and Krumlauf, R. (1989). The murine and Drosophila homeobox gene complexes have common features of organization and expression. *Cell* **57**, 367-378.

Grandel, H. and Brand, M. (2011). Zebrafish limb development is triggered by a retinoic acid signal during gastrulation. *Dev Dyn* **240**, 1116-1126.

Grandel, H., Lun, K., Rauch, G. J., Rhinn, M., Piotrowski, T., Houart, C., Sordino, P., Kuchler, A. M., Schulte-Merker, S., Geisler, R., et al. (2002). Retinoic acid signalling in the zebrafish embryo is necessary during pre-segmentation stages to pattern the anterior-posterior axis of the CNS and to induce a pectoral fin bud. *Development* **129**, 2851-2865.

Horan, G. S., Ramirez-Solis, R., Featherstone, M. S., Wolgemuth, D. J., Bradley, A. and Behringer, R. R. (1995). Compound mutants for the paralogous hoxa-4, hoxb-4, and hoxd-4 genes show more complete homeotic transformations and a dose-dependent increase in the number of vertebrae transformed. *Genes Dev* **9**, 1667-1677.

Iimura, T. and Pourquie, O. (2007). Hox genes in time and space during vertebrate body formation. *Dev Growth Differ* **49**, 265-275.

Ishizaka, M., Maeno, A., Nakazawa, H., Fujii, R., Oikawa, S., Tani, T., Kanno, H., Koita, R. and Kawamura, A. (2024). The functional roles of zebrafish HoxA- and HoxD-related clusters in the pectoral fin development. *Sci Rep* **14**, 23602.

Izpisua-Belmonte, J. C. and Duboule, D. (1992). Homeobox genes and pattern formation in the vertebrate limb. *Dev Biol* **152**, 26-36.

Janvier, P. (1996). Early Vertebrates.

Jurberg, A. D., Aires, R., Varela-Lasheras, I., Novoa, A. and Mallo, M. (2013). Switching axial progenitors from producing trunk to tail tissues in vertebrate embryos. *Dev Cell* **25**, 451-462.

Keegan, B. R., Feldman, J. L., Begemann, G., Ingham, P. W. and Yelon, D. (2005). Retinoic acid signaling restricts the cardiac progenitor pool. *Science* **307**, 247-249.

Kimmel, C. B., Ballard, W. W., Kimmel, S. R., Ullmann, B. and Schilling, T. F. (1995). Stages of embryonic development of the zebrafish. *Dev Dyn* **203**, 253-310.

Kmita, M., Tarchini, B., Zakany, J., Logan, M., Tabin, C. J. and Duboule, D. (2005). Early developmental arrest of mammalian limbs lacking HoxA/HoxD gene function. *Nature* **435**, 1113-1116.

Krumlauf, R. (1994). Hox genes in vertebrate development. *Cell* **78**, 191-201.

Langston, A. W. and Gudas, L. J. (1994). Retinoic acid and homeobox gene regulation. *Curr Opin Genet Dev* **4**, 550-555.

Le Mouellic, H., Lallemand, Y. and Brulet, P. (1992). Homeosis in the mouse induced by a null mutation in the Hox-3.1 gene. *Cell* **69**, 251-264.

Lewis, E. B. (1978). A gene complex controlling segmentation in Drosophila. *Nature* **276**, 565-570.

Maeno, A., Koita, R., Nakazawa, H., Fujii, R., Yamada, K., Oikawa, S., Tani, T., Ishizaka, M., Satoh, K., Ishizu, A., et al. (2024). The Hox code responsible for the patterning of the anterior vertebrae in zebrafish. *Development* **151**.

Mansour, S. L., Thomas, K. R. and Capecchi, M. R. (1988). Disruption of the proto-oncogene int-2 in mouse embryo-derived stem cells: a general strategy for targeting mutations to non-selectable genes. *Nature* **336**, 348-352.

Marshall, H., Morrison, A., Studer, M., Popperl, H. and Krumlauf, R. (1996). Retinoids and Hox genes. *FASEB J* **10**, 969-978.

McIntyre, D. C., Rakshit, S., Yallowitz, A. R., Loken, L., Jeannotte, L., Capecchi, M. R. and Wellik, D. M. (2007). Hox patterning of the vertebrate rib cage. *Development* **134**, 2981-2989.

Medina-Martinez, O., Bradley, A. and Ramirez-Solis, R. (2000). A large targeted deletion of Hoxb1-Hoxb9 produces a series of single-segment anterior homeotic transformations. *Dev Biol* **222**, 71-83.

Meeker, N. D., Hutchinson, S. A., Ho, L. and Trede, N. S. (2007). Method for isolation of PCR-ready genomic DNA from zebrafish tissues. *BioTechniques* **43**, 610, 612, 614.

Minguillon, C., Gibson-Brown, J. J. and Logan, M. P. (2009). Tbx4/5 gene duplication and the origin of vertebrate paired appendages. *Proc Natl Acad Sci U S A* **106**, 21726-21730.

Minguillon, C., Nishimoto, S., Wood, S., Vendrell, E., Gibson-Brown, J. J. and Logan, M. P. (2012). Hox genes regulate the onset of Tbx5 expression in the forelimb. *Development* **139**, 3180-3188.

Moreau, C., Caldarelli, P., Rocancourt, D., Roussel, J., Denans, N., Pourquie, O. and Gros, J. (2019). Timed Collinear Activation of Hox Genes during Gastrulation Controls the Avian

Forelimb Position. *Curr Biol* **29**, 35-50 e34.

Murata, Y., Tamura, M., Aita, Y., Fujimura, K., Murakami, Y., Okabe, M., Okada, N. and Tanaka, M. (2010). Allometric growth of the trunk leads to the rostral shift of the pelvic fin in teleost fishes. *Dev Biol* **347**, 236-245.

Neto, A., Mercader, N. and Gomez-Skarmeta, J. L. (2012). The Osr1 and Osr2 genes act in the pronephric anlage downstream of retinoic acid signaling and upstream of Wnt2b to maintain pectoral fin development. *Development* **139**, 301-311.

Ng, J. K., Kawakami, Y., Buscher, D., Raya, A., Itoh, T., Koth, C. M., Rodriguez Esteban, C., Rodriguez-Leon, J., Garrity, D. M., Fishman, M. C., et al. (2002). The limb identity gene Tbx5 promotes limb initiation by interacting with Wnt2b and Fgf10. *Development* **129**, 5161-5170.

Niederreither, K., Vermot, J., Messaddeq, N., Schuhbaur, B., Chambon, P. and Dolle, P. (2001). Embryonic retinoic acid synthesis is essential for heart morphogenesis in the mouse. *Development* **128**, 1019-1031.

Niederreither, K., Vermot, J., Schuhbaur, B., Chambon, P. and Dolle, P. (2002). Embryonic retinoic acid synthesis is required for forelimb growth and anteroposterior patterning in the mouse. *Development* **129**, 3563-3574.

Nishimoto, S. and Logan, M. P. (2016). Subdivision of the lateral plate mesoderm and specification of the forelimb and hindlimb forming domains. *Semin Cell Dev Biol* **49**, 102-108.

Nishimoto, S., Minguillon, C., Wood, S. and Logan, M. P. (2014). A combination of activation and repression by a colinear Hox code controls forelimb-restricted expression of Tbx5 and reveals Hox protein specificity. *PLoS Genet* **10**, e1004245.

Ohno, S. (1970). Evolution by gene duplication.

Ota, S., Hisano, Y., Muraki, M., Hoshijima, K., Dahlem, T. J., Grunwald, D. J., Okada, Y. and Kawahara, A. (2013). Efficient identification of TALEN-mediated genome modifications using heteroduplex mobility assays. *Genes Cells* **18**, 450-458.

Parichy, D. M., Elizondo, M. R., Mills, M. G., Gordon, T. N. and Engeszer, R. E. (2009). Normal table of postembryonic zebrafish development: staging by externally visible anatomy of the living fish. *Dev Dyn* **238**, 2975-3015.

Rancourt, D. E., Tsuzuki, T. and Capecchi, M. R. (1995). Genetic interaction between hoxb-5 and hoxb-6 is revealed by nonallelic noncomplementation. *Genes Dev* **9**, 108-122.

Rossi, A., Kontarakis, Z., Gerri, C., Nolte, H., Holper, S., Kruger, M. and Stainier, D. Y. (2015). Genetic compensation induced by deleterious mutations but not gene knockdowns. *Nature* **524**, 230-233.

Satoh, K., Maeno, A., Adachi, U., Ishizaka, M., Yamada, K., Koita, R., Nakazawa, H., Oikawa, S., Fujii, R., Furudate, H., et al. (2024). Physical constraints on the positions and

dimensions of the zebrafish swim bladder by surrounding bones. *J Anat*.

Serbedzija, G. N., Chen, J. N. and Fishman, M. C. (1998). Regulation in the heart field of zebrafish. *Development* **125**, 1095-1101.

Shimada, A., Kawanishi, T., Kaneko, T., Yoshihara, H., Yano, T., Inohaya, K., Kinoshita, M., Kamei, Y., Tamura, K. and Takeda, H. (2013). Trunk exoskeleton in teleosts is mesodermal in origin. *Nat Commun* **4**, 1639.

Shubin, N., Tabin, C. and Carroll, S. (1997). Fossils, genes and the evolution of animal limbs. *Nature* **388**, 639-648.

Sztal, T. E. and Stainier, D. Y. R. (2020). Transcriptional adaptation: a mechanism underlying genetic robustness. *Development* **147**.

Tanaka, M. (2013). Molecular and evolutionary basis of limb field specification and limb initiation. *Dev Growth Differ* **55**, 149-163.

Thisse, B. and Thisse, C. (2014). In situ hybridization on whole-mount zebrafish embryos and young larvae. *Methods Mol Biol* **1211**, 53-67.

Tickle, C. (2015). How the embryo makes a limb: determination, polarity and identity. *J Anat* **227**, 418-430.

van den Akker, E., Fromental-Ramain, C., de Graaff, W., Le Mouellic, H., Brulet, P., Chambon, P. and Deschamps, J. (2001). Axial skeletal patterning in mice lacking all paralogous group 8 Hox genes. *Development* **128**, 1911-1921.

Waxman, J. S., Keegan, B. R., Roberts, R. W., Poss, K. D. and Yelon, D. (2008). Hoxb5b acts downstream of retinoic acid signaling in the forelimb field to restrict heart field potential in zebrafish. *Dev Cell* **15**, 923-934.

Wellik, D. M. and Capecchi, M. R. (2003). Hox10 and Hox11 genes are required to globally pattern the mammalian skeleton. *Science* **301**, 363-367.

Wellik, D. M., Hawkes, P. J. and Capecchi, M. R. (2002). Hox11 paralogous genes are essential for metanephric kidney induction. *Genes Dev* **16**, 1423-1432.

Woltering, J. M. and Durston, A. J. (2006). The zebrafish hoxDb cluster has been reduced to a single microRNA. *Nat Genet* **38**, 601-602.

Xu, B., Hrycaj, S. M., McIntyre, D. C., Baker, N. C., Takeuchi, J. K., Jeannotte, L., Gaber, Z. B., Novitch, B. G. and Wellik, D. M. (2013). Hox5 interacts with Plzf to restrict Shh expression in the developing forelimb. *Proc Natl Acad Sci U S A* **110**, 19438-19443.

Yamada, K., Maeno, A., Araki, S., Kikuchi, M., Suzuki, M., Ishizaka, M., Satoh, K., Akama, K., Kawabe, Y., Suzuki, K., et al. (2021). An atlas of seven zebrafish hox cluster mutants provides insights into sub/neofunctionalization of vertebrate Hox clusters. *Development* **148**.

Yelon, D., Horne, S. A. and Stainier, D. Y. (1999). Restricted expression of cardiac myosin genes

reveals regulated aspects of heart tube assembly in zebrafish. *Dev Biol* **214**, 23-37.

Figure legends

Figure 1. Lack of pectoral fins in *hoxba;hoxbb* cluster-deleted mutants. (A-G) Dorsal views of live zebrafish larvae at 3 dpf, obtained from intercrosses between *hoxba;hoxbb* cluster-deficient hemizygous fish. Arrowheads indicate the positions of the pectoral fins. (H-M) Expression patterns of *tbx5a* in the pectoral fin bud (arrowhead) at 30 hpf. Dorsal views are shown, and the genotype of each specimen was determined. For each genotype, reproducibility was confirmed with at least three different specimens. Genotyping revealed that all the embryos lacking pectoral fins (*n*=15) were *hoxba;hoxbb* double homozygotes. Scale bars are 100 μm.

Figure 2. Significantly decreased expression of *tbx5a* in the pectoral fin buds is specific to *hoxba;hoxbb* cluster-deleted mutants.
(A-I) Expression patterns of *tbx5a* in the pectoral fin buds of combinatorial deletion mutants of zebrafish *hox* clusters. Dorsal views of embryos at 30 hpf are displayed. After capturing images, the genotype of each specimen was determined. For each genotype, reproducibility was confirmed with at least three different specimens. Scale bars are 100 μm.

Figure 3. Transformation of pectoral fin progenitor cells into cardiac cells in *hoxba;hoxbb* homozygous embryos. (A-F) Expression patterns of *tbx5a* were compared between sibling wild-type and *hoxba;hoxbb* homozygous embryos during embryogenesis. The range of *tbx5a* expression in the lateral mesoderm is indicated by a bracket. The progenitor cells of pectoral fins are indicated by an arrowhead. (G, H)

Expression patterns of *nkx2.5* were compared between sibling and *hoxba;hoxbb* mutants. Enlarged views are shown in (G', H'). The different regions of *nkx2.5* expression between wild-type and mutants are indicated by brackets. (I, J) Expression patterns of *cmlc2* are shown. All images were captured from the dorsal side. For each stage, reproducibility was confirmed with at least three different specimens. Scale bars indicate 100 μm.

Figure 4. Zebrafish *hoxba;hoxbb* mutants lack a response to RA in fin buds. (A-D) Exogenous RA exposure in *raldh2* mutants can rescue *tbx5a* expression in fin buds. Arrowheads indicate the positions of the pectoral fin buds. (E-H) RA treatments in *hoxba;hoxbb* cluster-deleted mutants do not rescue *tbx5a* expression in fin buds. (I, J) Expression patterns of *raldh2* were compared between sibling and *hoxba;hoxbb* mutants. For each genotype, reproducibility was confirmed with at least three different specimens. All images were captured from the dorsal side. Scale bars represent 100 μm.

Figure 5. The expression patterns of *hox5a* and *hoxb5b* are regulated by RA. (A) Schematic representation of the 49 *hox* genes organized into seven *hox* clusters in zebrafish. *hox* genes in *hoxba* and *hoxbb* clusters are highlighted with orange. (B) Expression profiles of the 49 *hox* genes in wild-type and *raldh2*$^{-/-}$ embryos at the 20-somite stage, analyzed by RNA-seq. The average FPKM of each *hox* gene was compared between sibling and *raldh2* mutants. The absence of specific *hox* genes is indicated by a slash. (C-H) Expression patterns of *hoxb5a* and *hoxb5b* in sibling wild-type, *raldh2*$^{-/-}$, and RA-treated *raldh2*$^{-/-}$ embryos at the 10-somite stage. Arrowheads indicate the presumptive positions of pectoral fin buds. For each genotype,

reproducibility was confirmed with at least three different specimens. All images are captured from the dorsal side. Scale bars represent 100 μm.

Figure 6. Screening for *hox* genes responsible for the specification of zebrafish pectoral fins.

(A) Schematic representation of the genetic screening for *hox* genes involved in the specification of pectoral fins in zebrafish. (B-G) Dorsal views of live mutant larvae at 3 dpf, were obtained during the screening. After capturing images, genotyping and DNA sequencing in target *hoxb* genes were conducted. For the mutants illustrated in (C-G), *hoxb* genes are shown with frameshift mutations introduced. Detailed information is provided in Supplementary Table S1. (H-J) Dorsal views of *hoxba*$^{-/-}$*;hoxb5b*$^{-/-}$ and *hoxba*$^{-/-}$*;hoxb5b*$^{-/-}$*;hoxb6b*$^{-/-}$ larvae at 3 dpf. (K-M) Expression patterns of *tbx5a* in *hoxba*$^{-/-}$*;hoxb5b*$^{-/-}$ and *hoxba*$^{-/-}$*;hoxb5b*$^{-/-}$*;hoxb6b*$^{-/-}$ mutants at 30 hpf. Arrowheads indicate the presumptive positions of pectoral fin buds. All images are captured from the dorsal side. Scale bars represent 100 μm.

Figure 7. *hoxb4a-b5a*$^{del/del}$*;hoxb5b*$^{del/del}$ larvae partially recapitulate the absence of the pectoral fins.

(A-C) Dorsal views of zebrafish *hoxba*$^{-/-}$*;hoxb5b*$^{del/del}$ larvae at 3 dpf. (D, E) Expression patterns of *tbx5a* in sibling wild-type and *hoxba*$^{-/-}$*;hoxb5b*$^{del/del}$ (n=4) at 30 hpf. Arrowheads indicate the presumptive positions of pectoral fin buds. (F, G) Dorsal view of frameshift-induced *hoxb5a*$^{-/-}$*;hoxb5b*$^{-/-}$ and *hoxb5a* $^{del/del}$*;hoxb5b*$^{del/del}$ larvae. (H) Expression patterns of zebrafish *hoxb4a* at the 10-somite stage. (I-K) Dorsal view of frameshift-induced *hoxb4a*$^{-/-}$*;hoxb5a*$^{-/-}$*;hoxb5b*$^{-/-}$ and *hoxb4a-b5a* $^{del/del}$*;hoxb5b*$^{del/del}$

larvae. All images are captured from the dorsal side. Arrowheads indicate the presumptive positions of pectoral fin buds. Scale bars represent 100 μm.

Figure S1. Generation of the zebrafish *raldh2* mutants by CRISPR-Cas9. (A) The nucleotide sequence surrounding the mutations in *raldh2* is shown on the left. The target sequence of the crRNA is emphasized with an underline, while the inserted nucleotide sequence is indicated in orange. Below the DNA sequence, the predicted amino acid is displayed, with red letters highlighting the abnormal amino acid resulting from the frameshift mutation. The asterisk represents the termination codon. (B) A schematic representation of the predicted protein structure is shown, with the red box indicating the abnormal amino acid sequences resulting from the frameshift mutations. The total number of predicted amino acids is displayed to the right of the schematic. (C) The absence of pectoral fins (arrowhead) in *raldh2* homozygous mutants is observed dorsally at 3 dpf. (D) The expression of *tbx5a* in the pectoral fin buds (arrowhead) is significantly reduced in *raldh2* mutants. The phenotype of our *raldh2*^{sud118} mutants closely resembles the phenotype observed in previously isolated *raldh2* mutants.

Figure S2. Volcano plot of the transcriptome analysis between sibling and *raldh2* mutants. The volcano plot illustrates both upregulated and downregulated differentially expressed genes from the comparison between wild-type and *raldh2* mutant embryos. Dot with more than a 2-fold increase in expression is indicated in orange, while those with more than a 2-fold decrease are shown in light blue. Among them, dots corresponding to *hox* genes are specifically highlighted.

Figure S3. Generation of the frameshift-induced *hox* mutants using CRISPR-Cas9. Schematic representations show zebrafish *hoxb8b*, *hoxb5b;hoxb6b*, and *hoxb5b;hoxb6b;hoxb8b* mutants. The other frameshift-induced *hox* mutants were previously described (Maeno et al., 2024). The nucleotide sequence around the mutations is shown on the left. The target sequence of crRNA is emphasized with an orange underline. The inserted nucleotide sequence is emphasized in red. Below the DNA sequence, the predicted amino acid is shown. Red letters indicate the abnormal amino acid caused by the frameshift mutation. On the right, a schema represents the predicted protein structure. The blue box indicates the homeodomain, and red box indicates the abnormal amino acid sequences from the frameshift mutations. The total number of the predicted amino acids is shown on the right of the schema.

Figure S4. Generation of locus-deletion mutants using CRISPR-Cas9. (A, C, E, G). Schematic representations show the genomic structure of zebrafish *hoxb4a*, *hox5a*, and *hoxb5b*. Boxes represent the exons, with the blue boxes indicating the coding regions. Black arrowheads indicate the target sites of crRNA, while red arrowheads represent the primers used for genotyping. (B, D, F, H) Display genomic locus deletions of *hox4a*, *hox5a*, *hoxb5b*, and *hoxb4a-b5a* deletion mutants. The flanking sequences of the 5’- and 3’- crRNA targets (underline) are shown in blue and green letters, respectively.

Figure 1

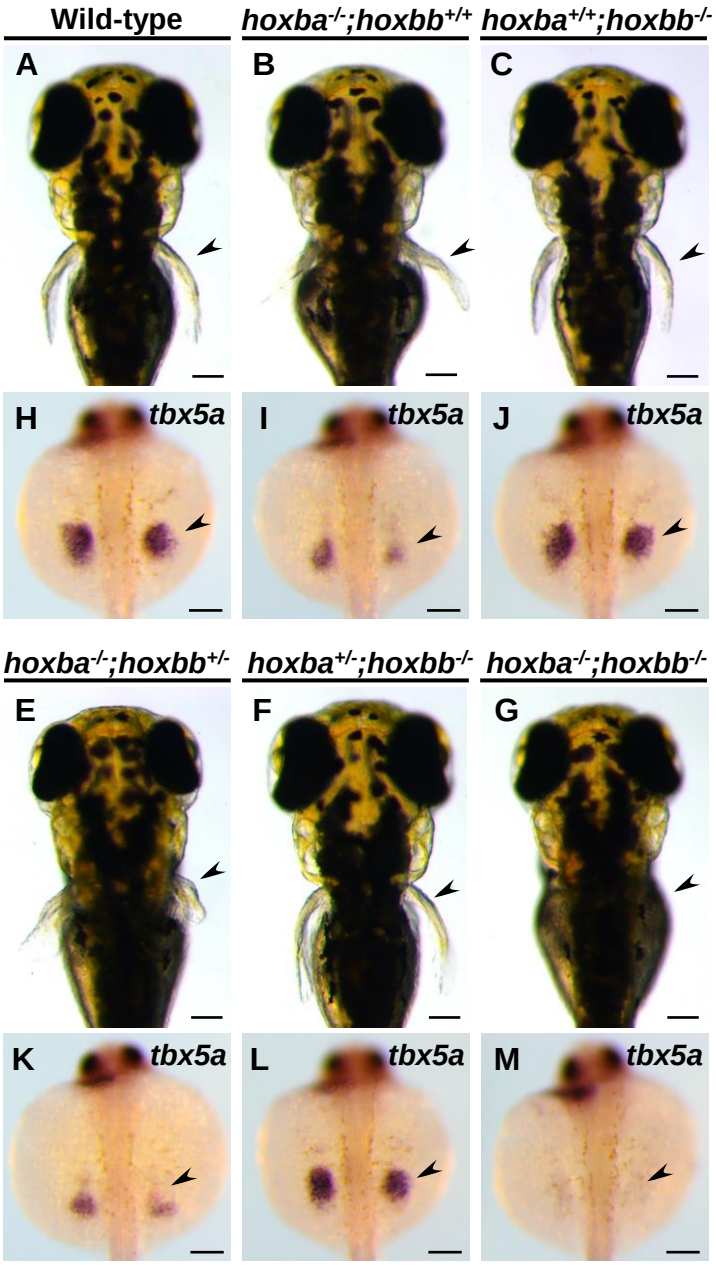

Figure 1. Lack of pectoral fins in *hoxba;hoxbb* cluster-deleted mutants. (A-G) Dorsal views of live zebrafish larvae at 3 dpf, obtained from intercrosses between *hoxba;hoxbb* cluster-deficient hemizygous fish. Arrowheads indicate the positions of pectoral fins. (H-M) Expression patterns of *tbx5a* in the pectoral fin bud (arrowhead) at 30 hpf. Dorsal views are shown capturing images, the genotype of each specimen was determined. For each genotype, reproducibility was confirmed with at least three different specimens. Genotyping revealed that all the embryos lacking pectoral fins (*n*=15) were *hoxba;hoxbb* double homozygotes. Scale bars are 100 μm.

Figure 2

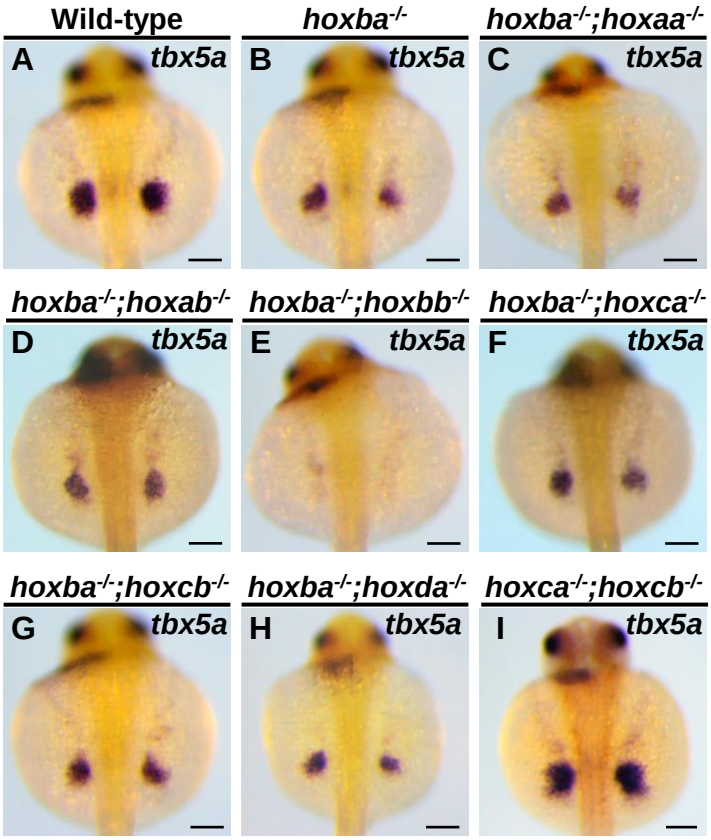

Figure 2. Significantly decreased expression of *tbx5a* in the pectoral fin buds is specific to *hoxba;hoxbb* cluster-deleted mutants.

(A-I) Expression patterns of *tbx5a* in the pectoral fin buds of combinatorial deletion mutants of zebrafish *hox* clusters. Dorsal views of embryos at 30 hpf are displayed. After capturing images, the genotype of each specimen was determined. For each genotype, reproducibility was confirmed with at least three different specimens. Scale bars are 100 μm.

Figure 3

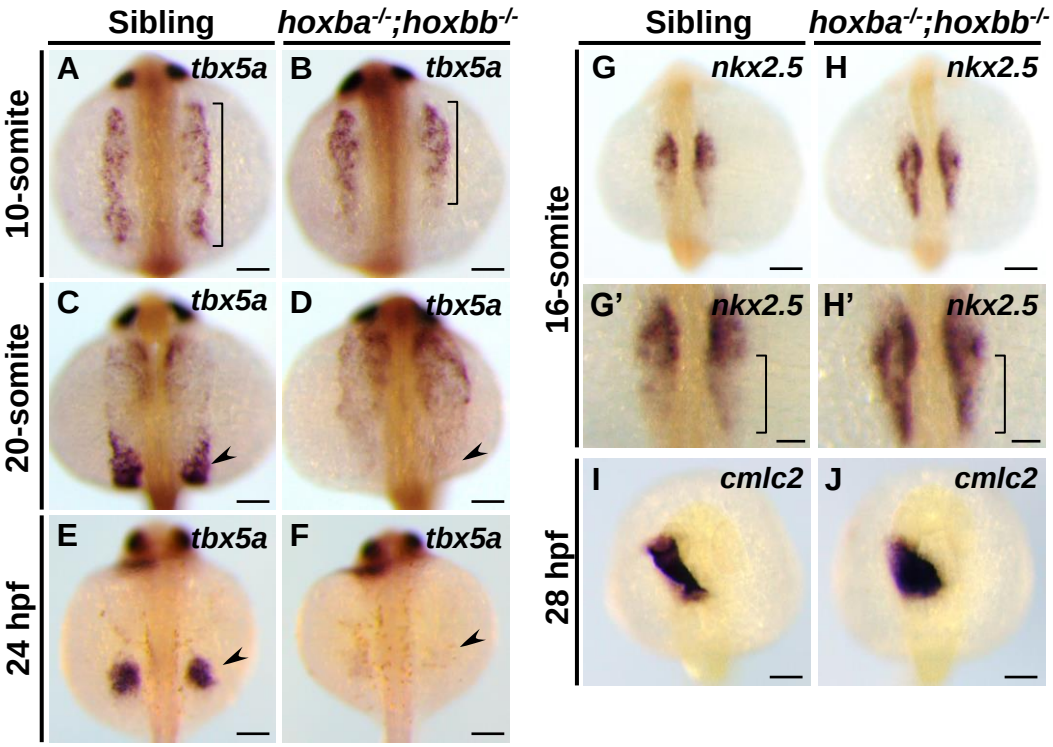

Figure 3. Transformation of pectoral fin progenitor cells into cardiac cells in *hoxba;hoxbb* homozygous embryos. (A-F) Expression patterns of *tbx5a* were compared between sibling wild-type and *hoxba;hoxbb* homozygous embryos during embryogenesis. The range of *tbx5a* expression in the lateral mesoderm is indicated by a bracket. The progenitor cells of pectoral fins are indicated by an arrowhead. (G, H) Expression patterns of *nkx2.5* were compared between sibling and *hoxba;hoxbb* mutants. Enlarged views are shown in (G', H'). The different regions of *nkx2.5* expression between the wild type and the mutant are indicated by brackets. (I, J) Expression patterns of *cmcl2* are shown. All images were captured from the dorsal side. Scale bars indicate 100 μm.

Figure 4

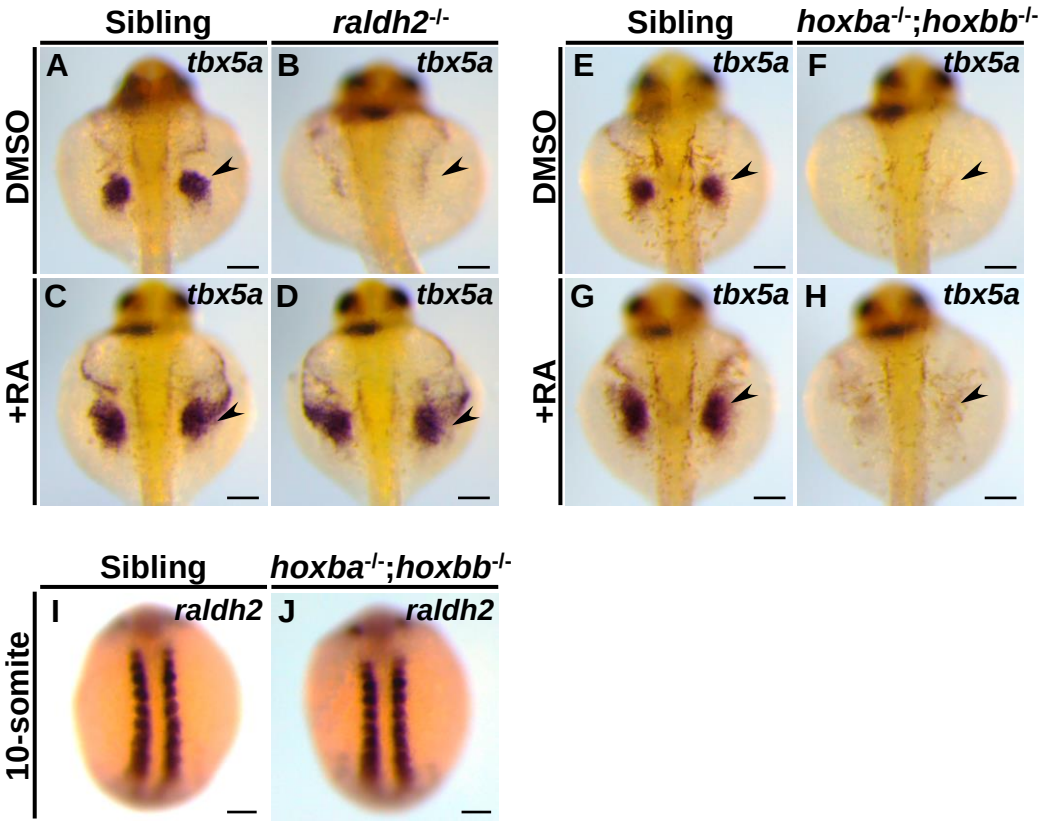

Figure 4. Zebrafish *hoxba;hoxbb* mutants lack a response to RA in fin buds. (A-D) Exogeneous RA exposure in *raldh2* mutants can rescue *tbx5a* expression in fin buds. Arrowheads indicate the positions of the pectoral fin buds. (E-H) RA treatments in *hoxba;hoxbb* cluster-deleted mutants do not rescue *tbx5a* expression in fin buds. (I, J) Expression patterns of *raldh2* were compared between sibling and *hoxba;hoxbb* mutants. All images were captured from the dorsal side. Scale bars represent 100 μm.

Figure 5

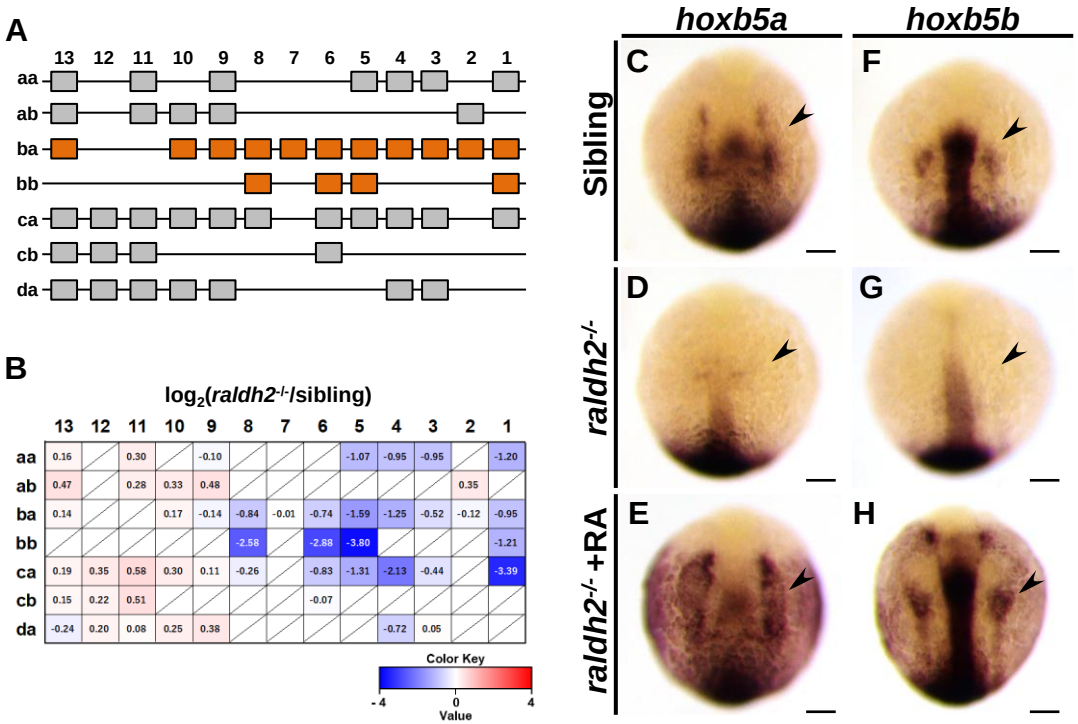

Figure 5. The expression patterns of *hox5a* and *hoxb5b* are regulated by RA. (A) Schematic representation of the 49 *hox* genes organized into seven *hox* clusters in zebrafish. *hox* genes in *hoxba* and *hoxbb* clusters are highlighted with orange. (B) Expression profiles of the 49 *hox* genes in wild-type and *raldh2*$^{-/-}$ embryos at the 20-somite stage, analyzed by RNA-seq. The average FPKM of each *hox* gene was compared between sibling and *raldh2* mutants. The absence of specific *hox* genes is indicated by a slash. (C-H) Expression patterns of *hoxb5a* and *hoxb5b* in sibling wild-type, *raldh2*$^{-/-}$, and RA-treated *raldh2*$^{-/-}$ embryos at the 10-somite stage. Arrowheads indicate the presumptive positions of pectoral fin buds. All images are captured from the dorsal side. Scale bars represent 100 μm.

Figure 6

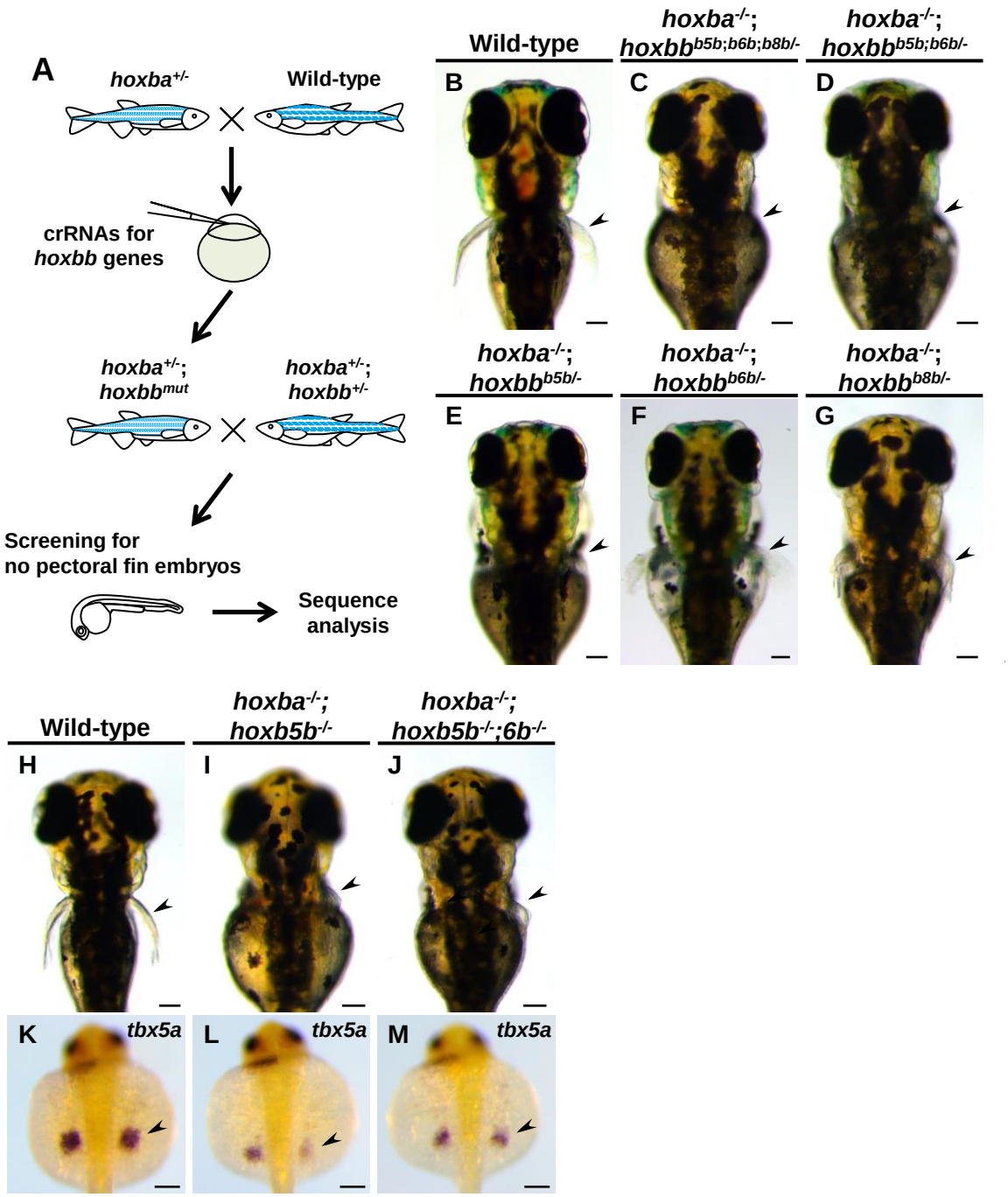

Figure 6. Screening for *hox* genes responsible for the specification of zebrafish pectoral fins.

(A) Schematic representation of the genetic screening for *hox* genes involved in the specification of pectoral fins in zebrafish. (B-G) Dorsal views of live mutant larvae at 3 dpf, obtained during the screening. After capturing images, genotyping and examination of mutations in *hoxb* genes were conducted. For the mutants illustrated in (C-G), *hoxb* genes are shown with frameshift mutations introduced. Detailed information is provided in Supplementary Table S1. (H-J) Dorsal views of l*hoxba*$^{-/-}$*;hoxb5b*$^{-/-}$ and *hoxba*$^{-/-}$*;hoxb5b*$^{-/-}$*;hoxb6b*$^{-/-}$ larvae at 3 dpf. (K-M) Expression patterns of *tbx5a* in *hoxba*$^{-/-}$*;hoxb5b*$^{-/-}$ and *hoxba*$^{-/-}$*;hoxb5b*$^{-/-}$*;hoxb6b*$^{-/-}$ mutants at 30 hpf. Arrowheads indicate the presumptive positions of pectoral fin buds. All images are captured from the dorsal side. Scale bars represent 100 μm.

Figure 7

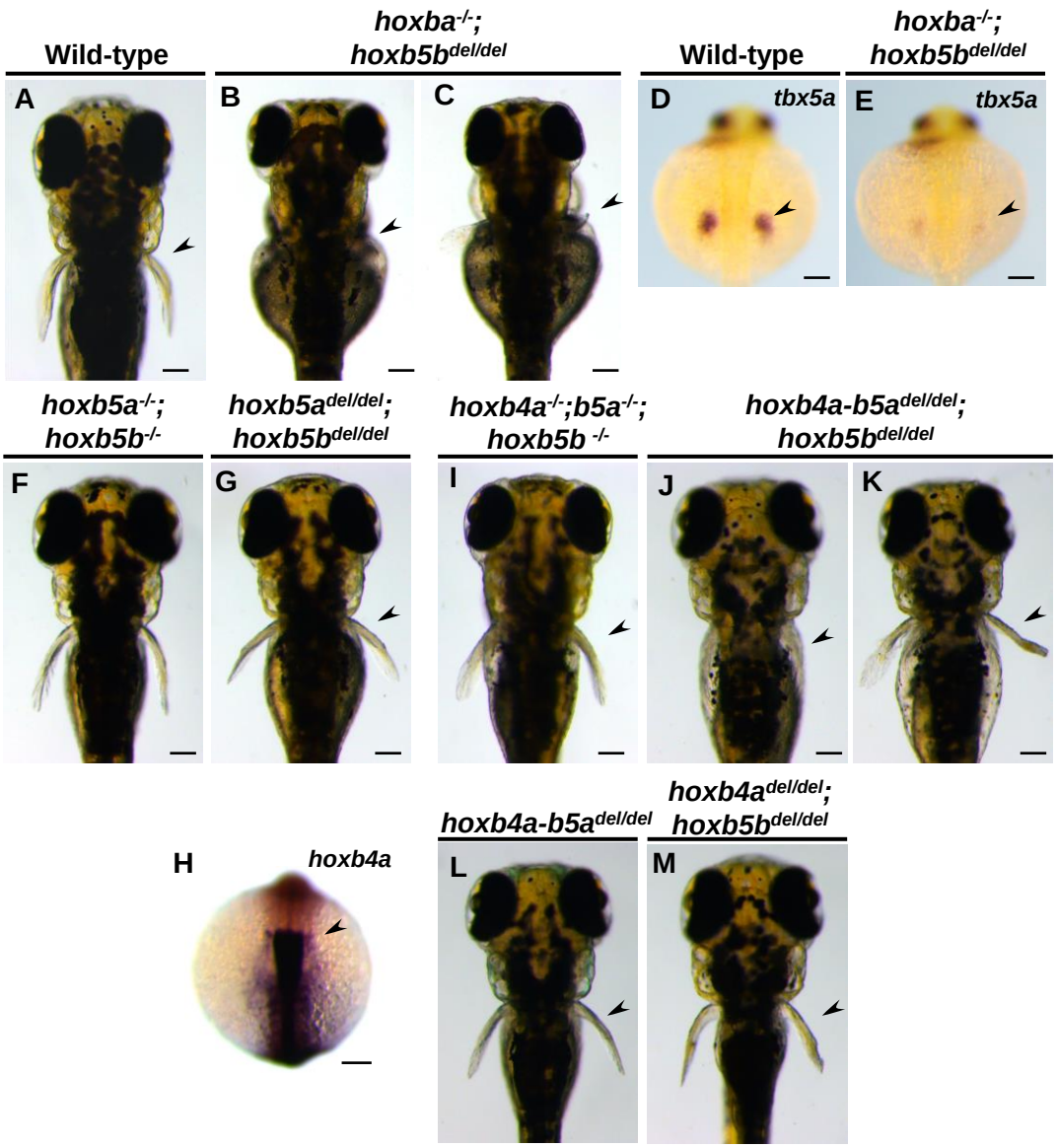

Figure 7. *hoxb4a-b5a*$^{del/del}$*;hoxb5b*$^{del/del}$ partially recapitulates the absence of the pectoral fins.

(A-C) Dorsal views of zebrafish *hoxba*$^{-/-}$*;hoxb5b*$^{del/del}$ larvae at 3 dpf. (D, E) Expression patterns of *tbx5a* in sibling wild-type and *hoxba*$^{-/-}$*;hoxb5b*$^{del/del}$ (*n*=4) at 30 hpf. Arrowheads indicate the presumptive positions of pectoral fin buds. (F, G) Dorsal view of frameshift-induced *hoxb5a*$^{-/-}$*;hoxb5b*$^{-/-}$ and *hoxb5a* $^{del/del}$*;hoxb5b*$^{del/del}$ larvae. (H) Expression patterns of zebrafish *hoxb4a* at the 10-somite stage. (I-M) Dorsal view of frameshift-induced *hoxb4a*$^{-/-}$*;hoxb5a*$^{-/-}$*;hoxb5b*$^{-/-}$, *hoxb4a-b5a* $^{del/del}$*;hoxb5b*$^{del/del}$, *hoxb4a-b5a* $^{del/del}$, and *hoxb4a* $^{del/del}$*;hoxb5b*$^{del/del}$ larvae. All images are captured from the dorsal side. Arrowheads indicate the presumptive positions of pectoral fin buds. Scale bars represent 100 μm.